Wing-Section Effects on the Flight Performance of a Remotely Piloted Vehicle

J. L. Stollery* and D. J. Dyer†
College of Aeronautics, Cranfield, Bedford, England, U.K.

Seven airfoil sections suitable for remotely piloted vehicles (RPV's) were tested at full-scale Reynolds numbers in the College of Aeronautics low-speed wind tunnel. The pressure distributions and force measurements were used to validate the mathematical model proposed by Williams. Three of the airfoils were further tested with roughness added. Of the airfoils tried, the Wörtman FX63-137 had the best performance. It was therefore decided to retrofit a wing of this section to an RPV designated X-RAE1. The original wing for this RPV had an unspecified flat-bottomed section, with a maximum thickness/chord ratio of 14.1% at the 30% chord station. First, a full-scale solid model of the X-RAE1 was tested in the Royal Aerospace Establishment 7.3 m tunnel. It was then retested with a new wing of the FX63-137 section, which gave substantial gains in $C_{L\max}$ and L/D ratio. Finally, a fully instrumented version of the X-RAE1 was constructed. Flight trials with the standard (flat lower surface) wing and with a new wing of the Wörtmann section confirmed the superiority of the FX63-137 airfoil. However, the flight tests also showed the large drag penalties due to the many practical features of a real flying vehicle.

Nomenclature

$\mathcal{R}$	= aspect ratio
C_D	= drag coefficient
C_L	= lift coefficient
C_p	= pressure coefficient
c	= mean chord
D	= drag
K	= roughness height
L	= lift
Re_c	= Reynolds number based on wing mean chord, Uv/c
t	= airfoil thickness
U_0	= test velocity or flight speed
x	= streamwise coordinate
α	= incidence relative to the true chord line of the wing section
α_1	= incidence relative to the fuselage datum, $=\alpha_1+2.5$ deg)
v	= kinematic viscosity of air

I. Introduction

THE Royal Aerospace Establishment (RAE) at Farnborough has been developing a series of small remotely piloted vehicles (RPV's) with a wing mean chord of typically 0.3 m. At a flying speed of between 20 and 50 m/s, the relevant Reynolds numbers are between 3×10^5 and 1.0×10^6. Wind-tunnel measurements in this range are relatively sparse. Under a Ministry of Defence (MoD) contract, experimental data on seven different smooth airfoils were obtained by Render.[1] The sections tested were the Göttingen 797, NACA64_3-418, and Wörtmann FX63-137, plus four modified Wörtmann sections in which the undercamber was progressively reduced. All of the sections tested are shown in Fig. 1a.

Davidson[2] repeated some of Render's tests in the same wind tunnel before going on to investigate the effects of roughness bands placed close to the leading edge on both upper and lower surfaces. Davidson concentrated on the three unmodified airfoils (NACA64_3-418, Göttingen 797, and FX63-137). As a result of these investigations, the RAE built a full-scale solid model of their RPV called X-RAE1 (see Fig. 3) and tested it in the 7.3 m low-speed open jet tunnel at Farnborough. The wing had an unspecified section with a flat lower surface and a maximum thickness/chord ratio of 14.1% at 30% chord. The model was then retested with a new wing of the FX63-137 section. The report by Trebble[3] showed the new wing to be better.

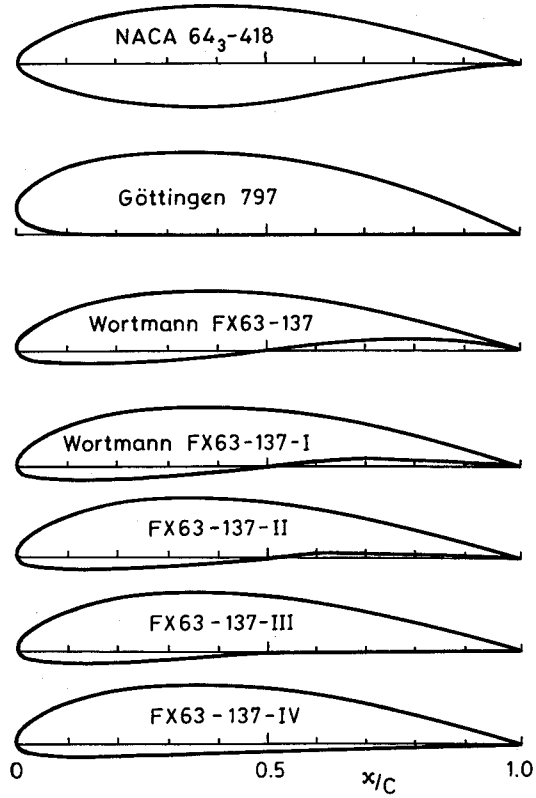

Fig. 1a The seven wind-tunnel tested airfoils.

Presented as Paper 88-4.9.2 at the 16th Congress of the International Council of the Aeronautical Sciences, Jerusalem, Israel, Aug. 28-Sept. 2, 1988; received Dec. 10, 1988; revision received March 22, 1989.

*Professor. Fellow AIAA.
†Senior Project Engineer.

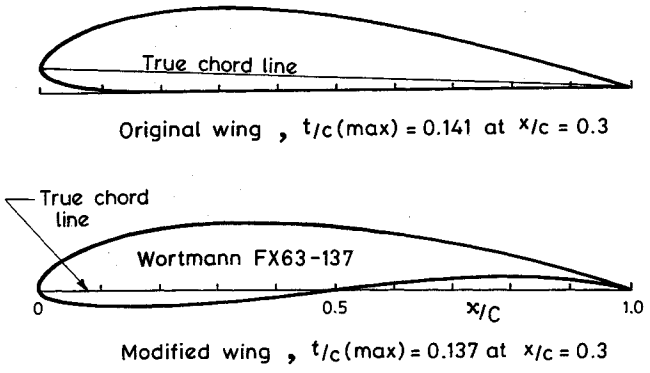

Fig. 1b The wing sections for X-RAE 1, both wings mounted with true chord line 2.5-deg nose up to fuselage datum.

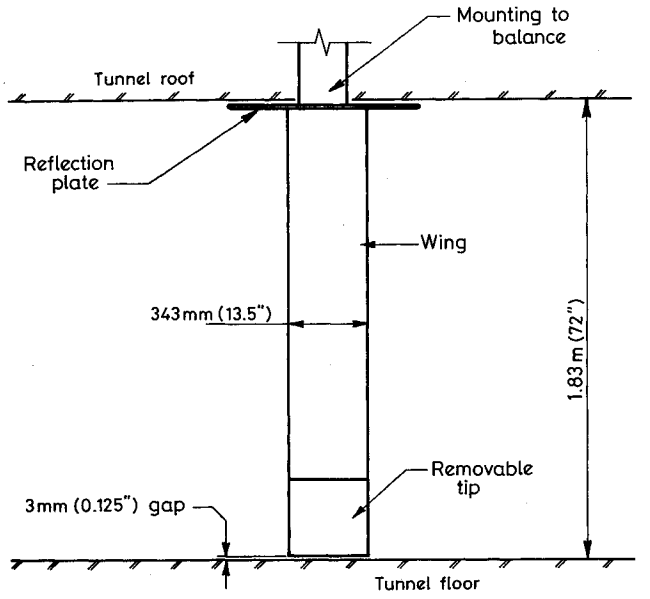

Fig. 2 Experimental arrangement in 2.44×1.83-m (8×6-ft) low-speed wind tunnel.

The final step in the investigation was to undertake flight trials of a fully instrumented RPV using each of the two wings. The flight trials were made at Cranfield during 1987 and the results are given here.

II. Experimental Details

The wind-tunnel measurements were made in the College of Aeronautics 8×6-ft (2.4×1.8-m), closed-working-section, closed-return, low-speed facility at velocities between 10 and 45 m/s. The experimental arrangement is shown in Fig. 2. The quasi-two-dimensional tests were made with the constant-chord model reaching from roof to floor with a 3-mm gap at the lower end. This gap enabled force measurements to be made using the overhead six-component electromechanical balance. A removable tip section converted the model into a three-dimensional half-wing of known aspect ratio.

Tests were made at Reynolds numbers (based on the wing chord of 343 mm) of 3×10^5, 5×10^5, 7×10^5, and 1×10^6.

The models were made of wood and had a smooth polished finish. In this condition, there were large areas of laminar flow over both the top and bottom surfaces.[1] Under real conditions, the leading edge of an RPV wing is likely to become roughened and in order to measure the likely degradation of performance some of the test were repeated with roughness strips added.

The roughness used was a 13-mm (½ in.) band of 100 grit sandpaper with adhesive backing. The band was placed near the leading edge (between 0.04 and 0.08x/c) on both upper and lower surfaces. Although the grit size was only 0.15 mm, the average height of the grit including the paper backing was 0.53 mm, and it was probably the "steps" at the leading and trailing edges of the roughness band that promoted transition.

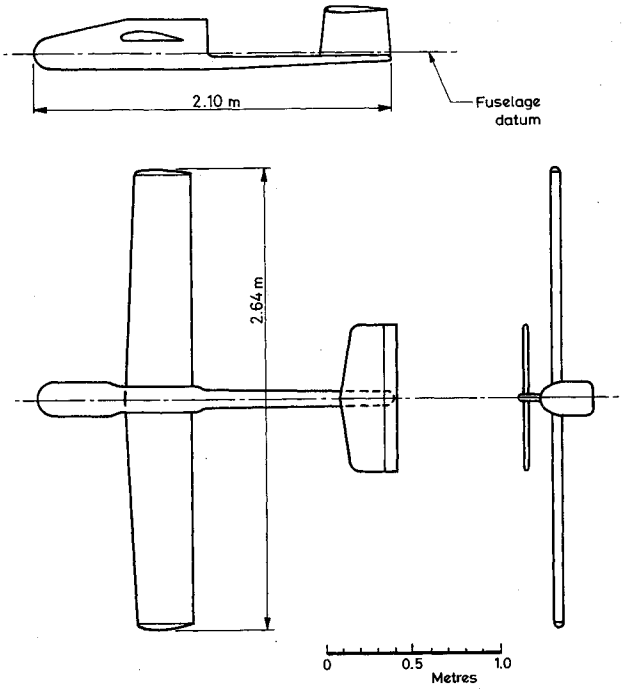

Fig. 3 Wind-tunnel model of X-RAE1 with rounded tips.

The roughness criterion given by Schlichting[4] states that for transition to be at the roughness station the roughness height K must exceed $900\nu/U$ (i.e., $K/c > 900/Re_c$). Given $K=0.53$ mm and $c=343$ mm, this means that Re_c should exceed 0.58×10^6. This suggests that for the tests at $Re_c=3\times10^5$ reported here, transition will have been promoted but may not have occurred at the roughness station.

Force and moment measurements were made using the six-component balance located above the tunnel roof. A Betz manometer measured and monitored the wind-tunnel test velocity.

The pressure measurements used about 40 ports in each surface, coupled via Scanivalves to Setra or Furness pressure transducers. The pressure ports were in a single line near the midspan position. They were sealed with wax when force measurements were being made.

The conditions in the wind-tunnel test section are known to be particularly important for tests at low Reynolds numbers. Recent measurements along the tunnel test section centerline indicated a turbulence intensity of 0.07% at a freestream velocity of 20 m/s rising to 0.14% at 50 m/s. Spectra taken for the frequency range 0–1000 Hz showed no obvious peaks, which suggests that the turbulence is small scale and covers a broad-band of frequencies.

Further details of the test procedures and wind-tunnel corrections are given in the work of Render[1] and Davidson.[2]

The wind-tunnel tests made at RAE Farnborough used a smooth, solid, wooden full-scale model of X-RAE1, as drawn in Fig. 3. The model was wire mounted in an inverted position from the overhead balance in the RAE 24 ft (7.3 m) diam open-jet low-speed wind tunnel. Lift, drag, and pitching moment measurements were made at velocities of 20, 30, 40, and 50 m/s with the original wing (whose section is shown in Fig. 1b) and with a wing of the FX63-137 section (see Fig. 1a).

The full-scale flight trials were conducted in the airfield at Cranfield. An alternative wing of the FX63-137 section was built using the same materials and techniques as the original (wooden spars and ribs completely enveloped in a plywood skin).

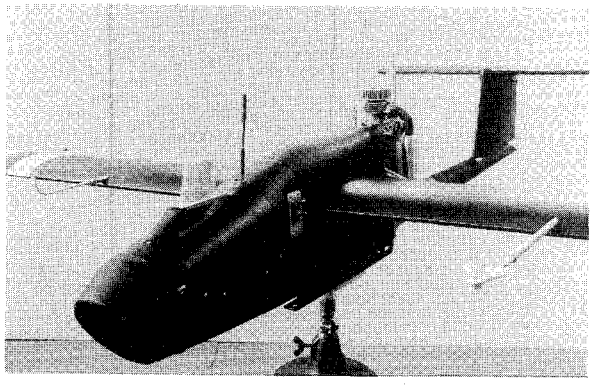

Fig. 4 The X-RAE1 RPV ready for flight trials.

The aircraft used for the flight tests is shown in Fig. 4, and some of the changes needed to carry the instrumentation are immediately apparent (e.g., a large fairing on top of the nose and booms mounted from both wings).

Although the wing and tail are of all-wood construction, the fuselage is a mixture of wood and glass fiber. The wing span is 2.7 m and the launch weight 17.0 kg. Power is supplied by a Webra 91 two-stroke engine producing 1.1 kW at 10,500 rpm.

The aircraft is fitted with the Cranfield Digital Flight Control System (DFCS), which was designed and developed under an earlier MoD (PE) contract. The DFCS consists of a telecommand receiver to receive uplink signals from the ground station, a 16-bit digital flight control computer (FCC), and a telemetry encoder for generation of downlink data for transmission from the aircraft to the ground station.

Sensors used in the aircraft are as follows: a J-TEC true airspeed sensor (TAS) is mounted in the nose fairing. The TAS operates by counting the vortices shed from a strut, the frequency being proportional to true airspeed.

The boom from the starboard wing carries a Prosser airspeed sensor, which operates on the hot-wire anemometer principle. An angle-of-attack vane is mounted forward of the port wing on a boom extending from the wing leading edge.

Accurate calibration of the airspeed and angle-of-attack sensors was of vital importance to the flight trials. Calibration of both airspeed sensors and of the angle-of-attack vane was carried out using two of Cranfield's low-speed wind tunnels. The J-TEC TAS was calibrated in place on the aircraft with the engine both running and static. The Prosser Sensor and the angle-of-attack vane were calibrated individually, the results being corrected using data from the RAE 24-ft tunnel tests.

A sensitive barometric pressure sensor (designed and manufactured at Cranfield) is used to provide both absolute pressure data and subsequently height data, after processing in the DFCS.

Engine rpm are measured using an optical sensor to provide a pulse input to the DFCS which effectively counts the signals.

A three-axis rate gyro pack, using Smiths Industries type 902 gyros, measures angular velocity of the aircraft in roll, pitch, and yaw.

The aircraft controls are ailerons, elevator, rudder, throttle, and airbrakes. The software installed for the flight trials provides three-axis rate stabilization, angle-of-attack-acquire and height-acquire modes.

The UHF telemetry downlink is received in the mobile ground station (a Ford Transit 22cwt LWB van) and recorded, together with telecommand data, time data, and voice communications, on a Racal Store 7 tape recorder.

The flight trials consisted of several flights to carry out long straight descents, using idle power, from typically 300 m down to 100 m.

Postflight analysis of the recorded data used angle of attack, true airspeed, barometric pressure, height, air temperature, time, and rpm information (and hence the thrust from propeller calibration data), along with the aircraft particulars.

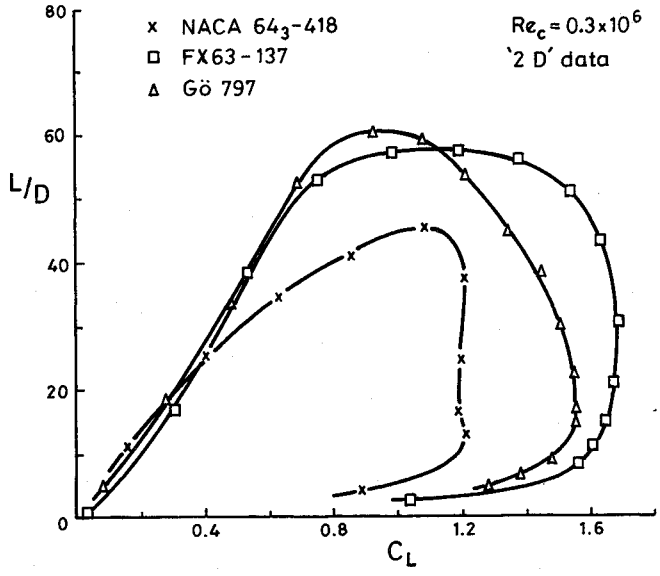

Fig. 5a Lift-drag ratios for the three wings.

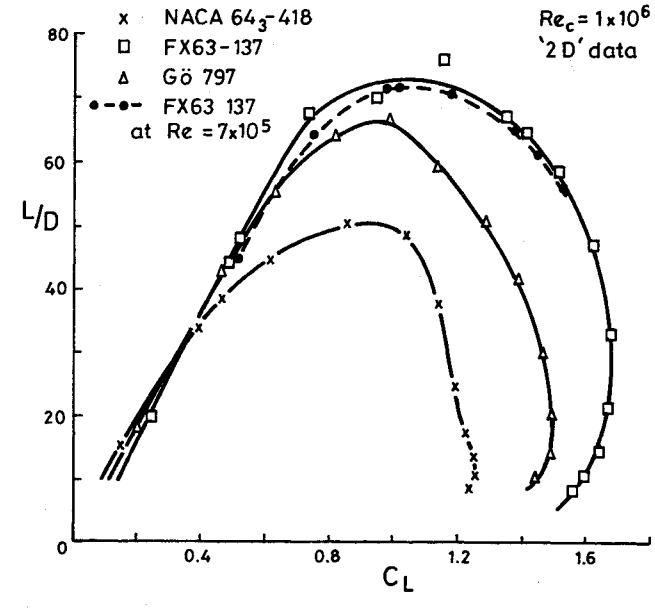

Fig. 5b Lift-drag ratios for the three wings.

III. Results and Discussion

The "two-dimensional" data on seven airfoils are summarized in Figs. 5 and 6. At $Re_c = 3 \times 10^5$, the Göttingen and Wörtmann sections have a similar L/D ratio at lift coefficients up to about 1.2 (Fig. 5a), but the Wörtmann section has a higher $C_{L\max}$. At the higher Re_c of 1×10^6, the Wörtmann section is clearly superior (Fig. 5b). To help draw a curve through somewhat scattered data in the vicinity of the maximum (L/D) region for the FX 63-137 section, the experimental data at $Re_c = 7 \times 10^5$ are also shown for this airfoil.

The good performance of the Göttingen section is partly attributable to the flat bottom. This supports a zero pressure gradient therefore maintaining entirely laminar flow over the lower surface at these Reynolds numbers. It was therefore decided to modify the FX 63-137 section by progressively flattening the lower surface as shown in Fig. 1a. The results (Fig. 6) show that the L/D ratios are slightly increased in the range $0 < C_L < 0.7$, the maximum (L/D) valves are much the same, but that $C_{L\max}$ is progressively lost as the undersurface is flattened.

The two-dimensional $C_{L\max}$ values as measured by Render on a smooth model are given in Table 1. The variation with

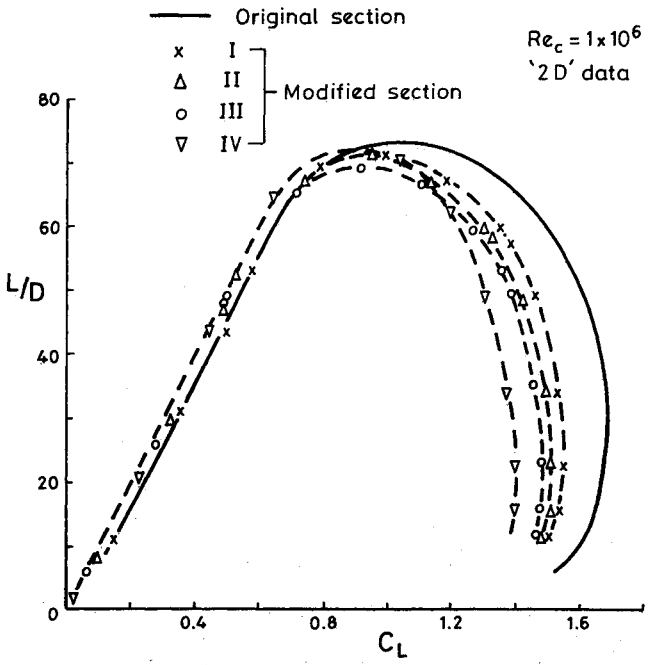

Fig. 6 Lift-drag ratios for the original and modified versions of FX63-137.

Re_c is quite small. In fact, the entire C_L-α curve changes little with Re_c within the range tested. However, the drag coefficients do change, decreasing progressively with increasing Re_c. This means that the L/D ratios improve with Re_c as can be seen by comparing Figs. 5a and 5b.

By analyzing all of the Render data, it became clear that of the seven airfoils tested the unmodified FX63-137 section was preferable. The lift-drag ratios were good throughout the C_L range, the maximum L/D values were similar to or better than any others measured, the maximum lift coefficient was the best recorded, and $C_{L\max}$ changes very little throughout the range of Reynolds numbers of interest.

Davidson[2] studied the question of performance degradation due to roughness. Some typical results are shown in Fig. 7 at

Table 1 Maximum lift coefficients measured from quasi-two-dimensional tests in the 8×6-ft. wind tunnel[1]

	Re_c			
Section	3×10^5	5×10^5	7×10^5	1×10^6
NACA64_3-418	1.21	1.22	1.24	1.26
Gö797	1.56	1.55	1.52	1.49
FX63-137	1.69	1.69	1.68	1.68
FX63-137 I	1.64	1.57	1.55	1.55
FX63-137 II	1.59	1.53	1.52	1.51
FX63-137 III	1.57	1.51	1.49	1.48
FX63-137 IV	1.49	1.44	1.41	1.40

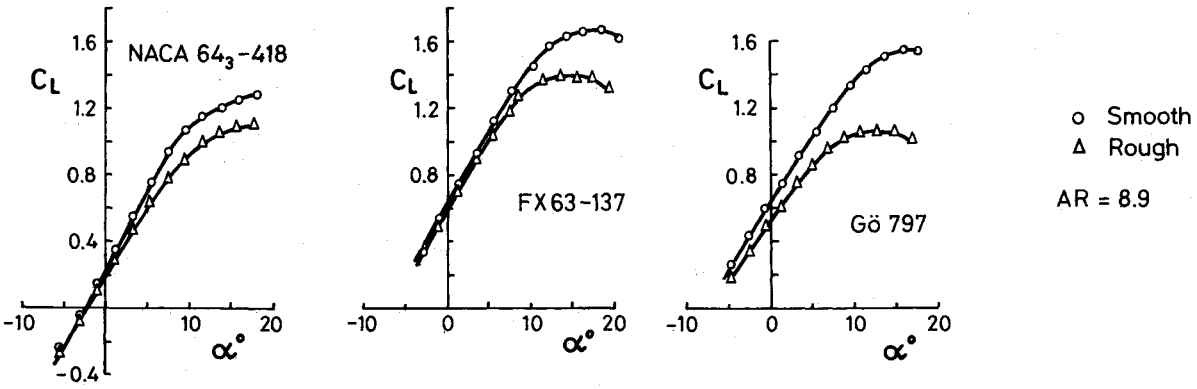

Fig. 7a Effect of roughness on lift for three airfoils at $Re_c = 1\times10^6$.

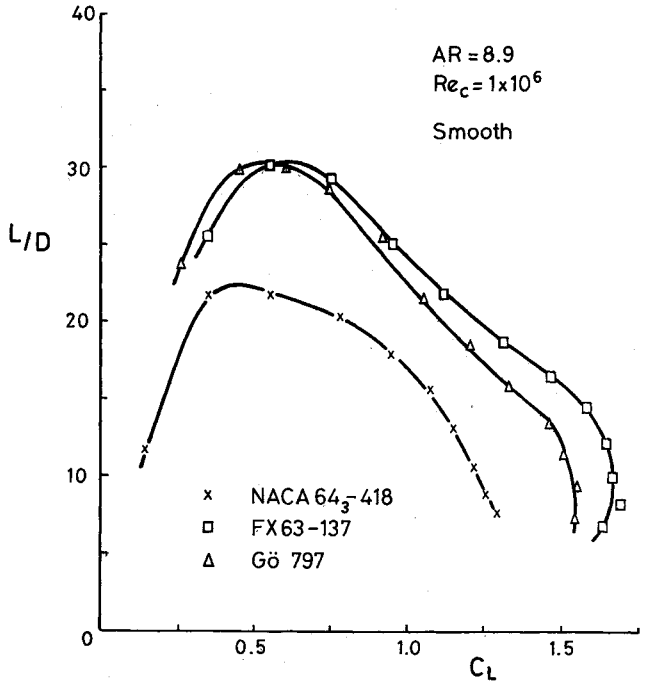

Fig. 7b Lift-drag ratios for the smooth wings.

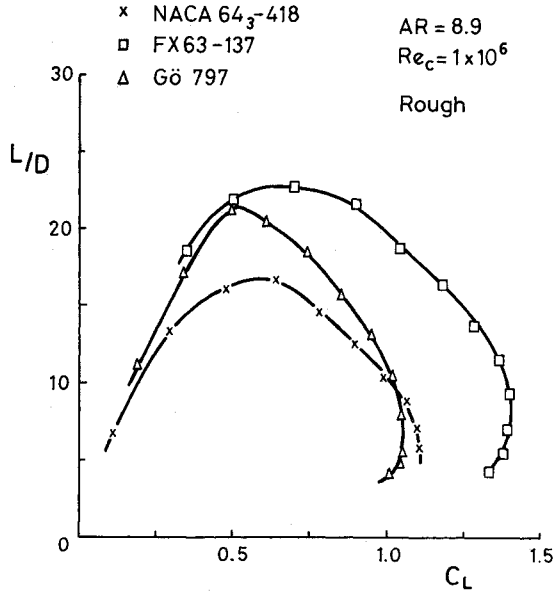

Fig. 7c Lift-drag ratios for the rough wings.

$Re_c = 1 \times 10^6$. This time the tip sections have been removed giving the characteristics shown in Table 2.

The measurements made with Göttingen 797 (Gö797) have been corrected to an aspect ratio of 8.9 so that sensible comparisons can be made.

Table 2

Wing Section	$NASA64_3$-418	FX63-137	Göttingen 797
Chord	343 mm (13.5 in.)	343 mm (13.5 in.)	343 mm (13.5 in.)
Semispan	1.523 m (60 in.)	1.423 m (60 in.)	1.366 m (53.8 in.)
Effective AR	8.9	8.9	8.0

Table 3 Maximum lift coefficients measured from finite aspect ratio half-model tests in the 8×6-ft wind tunnel[2]

	Section					
	$NACA64_3$-418 $\mathcal{R}=8.9$		Göttingen 797 $\mathcal{R}=8.0$		FX63-137 $\mathcal{R}=8.9$	
Re_c	Smooth	Rough	Smooth	Rough	Smooth	Rough
3×10^5	1.25	1.13	1.59	1.13	1.67	1.51
5×10^5	1.25	1.11	1.57	1.08	1.64	1.50
7×10^5	1.27	1.10	1.55	1.05	1.68	1.41
1×10^6	1.30	1.11	1.55	1.05	1.68	1.41

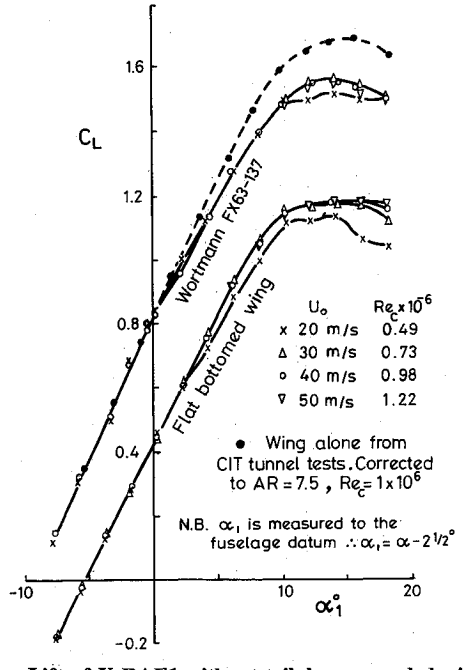

Fig. 8a Lift of X-RAE1 without tailplane, rounded wing tips.

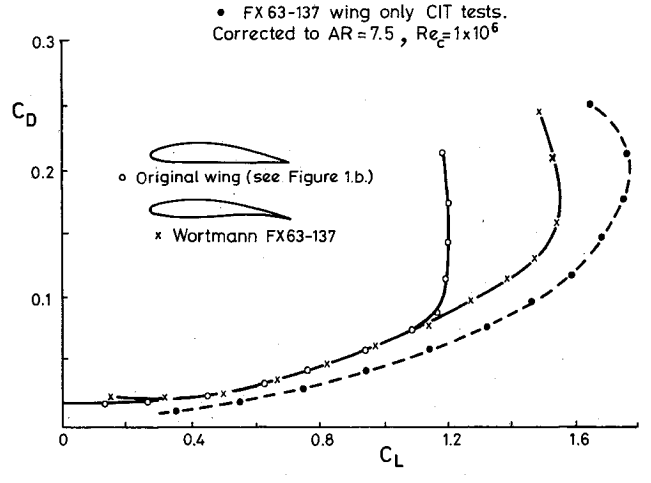

Fig. 8b Drag of X-RAE1 without tailplane, rounded wing tips, $U_0 = 40$ m/s.

Figure 7a shows that $C_{L\max}$ is significantly reduced by roughness and the Gö797 section is the most affected. Figure 7b confirms the two-dimensional smooth data in which the FX63-137 wing has higher lift/drag ratios than the Gö797 at the large C_L and both are superior to the NACA section. The superiority of the Wörtmann section is even clearer for the "rough" airfoils. The roughness strips promoting earlier transition lead to much earlier separation of the turbulent boundary layer on the top surface of the Göttingen section.

The values of $C_{L\max}$ for the rough and smooth wings at an aspect ratio of 8.9 are given in Table 3. Comparison with Table 1 suggests there is a little loss of $C_{L\max}$ with aspect ratio in the range 8.9 to "infinity."

Because the Wörtmann section looked so promising, Trebble[3] carried out tests on the experimental RPV designated X-RAE1. The characteristics of the vehicle are given in Fig. 3 and the original wing section in Fig. 1b.

Some results from Trebble's[3] report are shown in Fig. 8. Although the drag results are similar (in fact both models have the same drag over the C_L range 0.2–1.0), the gain in $C_{L\max}$ from the Wörtmann section is dramatic. For comparison, some estimates from our tunnel data for a wing alone with the same aspect ratio as the X-RAE model are included. The loss of $C_{L\max}$ due to wing-body interference is clearly visible, and the drag increase due to fuselage drag, fin drag, and interference drag is very significant.

Finally, the flight data are shown in Fig. 9 in comparison with Trebble's wind-tunnel measurements. The C_L values are

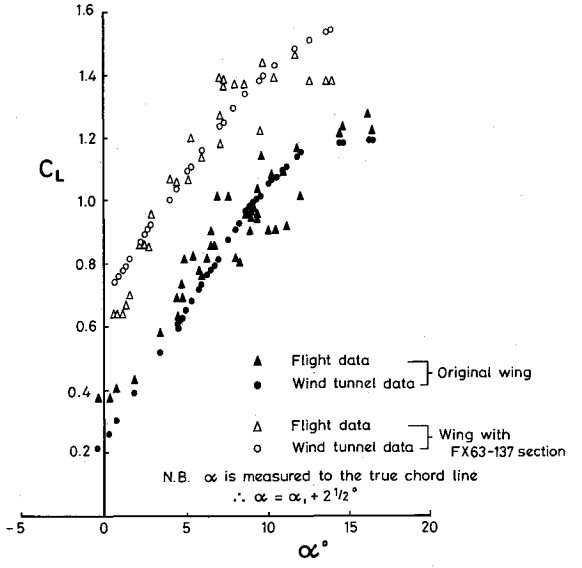

Fig. 9a Comparison between flight and wind-tunnel data for X-RAE1.

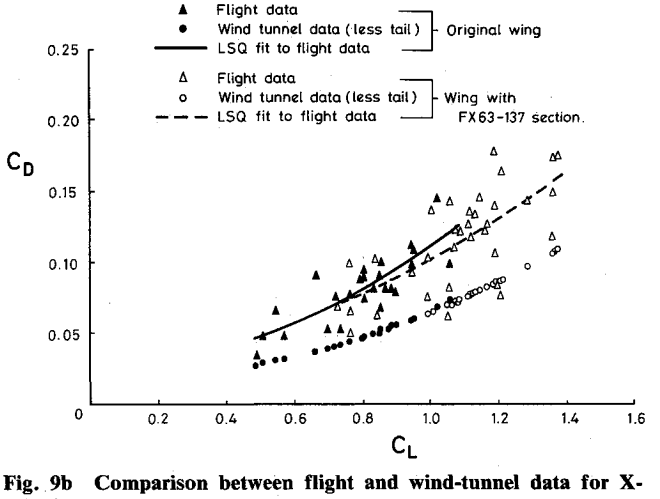

Fig. 9b Comparison between flight and wind-tunnel data for X-RAE1.

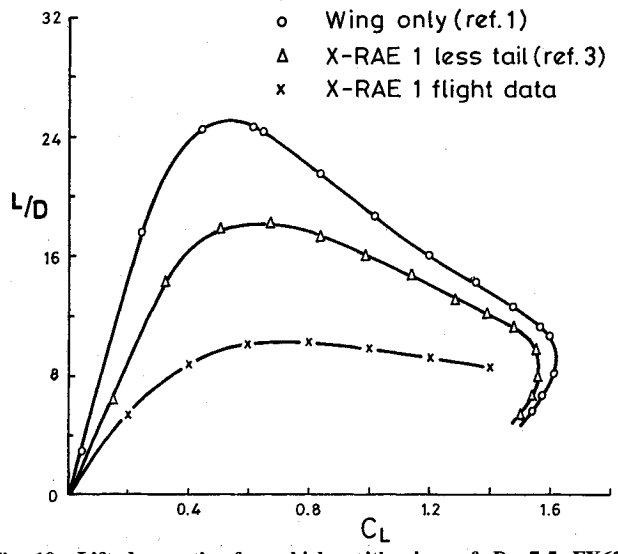

Fig. 10 Lift-drag ratios for vehicles with wings of $\mathcal{R}=7.5$, FX63-137 section, and $Re_c = 1\times10^6$.

for the complete model in the trimmed condition, whereas the C_D tunnel values are tail off although this would only account for a small drag difference in comparison with the flight values.

The first thing to notice is the scatter in the flight data. Great care was taken but flight measurements are infinitely more difficult than those made in the well-controlled environment of the wind tunnel. In particular, it is very difficult to measure $C_{L\max}$ in flight. Nevertheless, the flight data (Fig. 9a) confirm most of the C_L–α curves measured in the RAE tunnel, and the benefit in $C_{L\max}$ in flight is clearly demonstrated.

The drag values measured in flight show a large scatter and a least-squares fit has been made to the data. Figure 9 shows that the flight drag values are considerably greater than the tunnel values and reference to Figs. 3 and 4 shows why. The flying vehicle had a much blunter nose, with a large airspeed sensor mounted in a fairing on top, instrumentation booms on both wings, cut outs, excrescences, propeller interference, engine cooling drag, tail drag, and trim drag. The result is that the flight values are nearly double the tunnel values. A real production RPV would not have all of the "instrumentation drag" of our vehicle so the comparison is a harsh one. Nevertheless, the comparison in Fig. 9b serves to highlight the very real differences between actual flight vehicles and smooth wind-tunnel models. To emphasize the point, Fig. 10 shows the L/D vs C_L plot for a rectangular wing-alone of aspect ratio 7.5, the tail-off data of Trebble, and the flight data measured at Cranfield. The wing section is the Wörtmann FX63-137 for all of the data shown. Starting with a clean wing only, the $(L/D)_{\max}$ is around 25. This reduces to about 18 for the smooth wind-tunnel model of the complete vehicle (less tail), whereas the actual experimental example of X-RAE1 in flight only achieves a value of 10.

The values of $C_{L\max}$ for the various configurations are given below for the Wörtmann airfoil FX63-137 at $Re_c = 1\times10^6$:

Two-dimensional wind-tunnel value (smooth)	$=1.68$
$\mathcal{R}=8.9$ wind-tunnel value (smooth)	$=1.68$
$\mathcal{R}=8.9$ wind-tunnel value (rough)	$=1.40$
Full-scale model of X-RAE1	$=1.55$
Flight data	$=1.45$

IV. Comparisons Between Theory and Experiment

The computational program uses an integral boundary-layer method that has been extended to calculating separated flow by assuming a two-parameter description of the separated profiles. The program is of the semi-inverse type in which a direct inviscid calculation is coupled to an inverse calculation of the boundary layer.

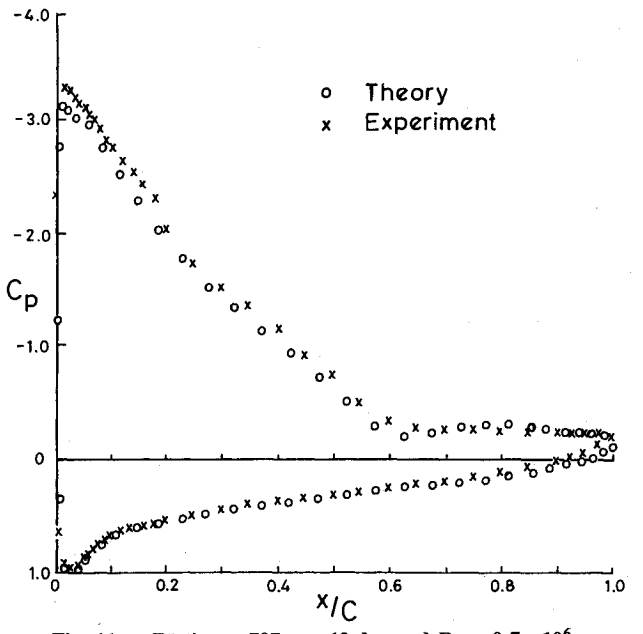

Fig. 11a Göttingen 797: $\alpha = 12$ deg and $Re_c = 0.7\times10^6$.

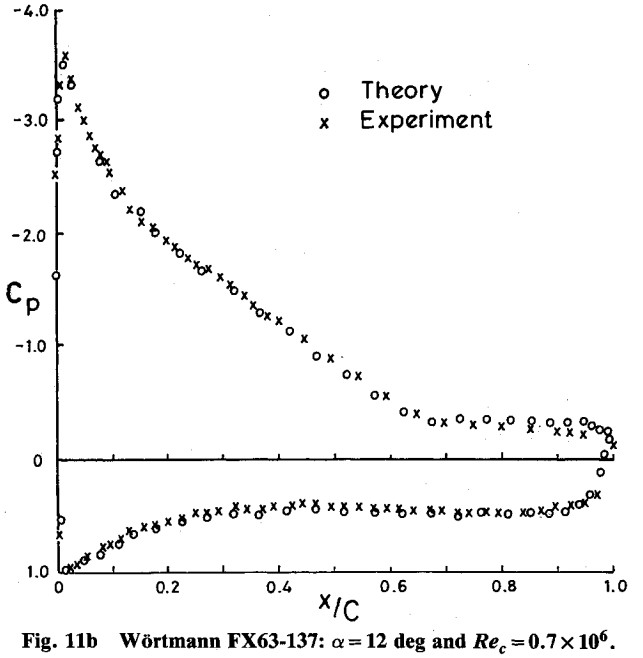

Fig. 11b Wörtmann FX63-137: $\alpha = 12$ deg and $Re_c = 0.7\times10^6$.

The outer inviscid flow is assumed here to be both incompressible and irrotational so that it can be described by the relevant solution of Laplace's equation.

The inner viscous flow is more difficult. The laminar portion of the boundary layer is calculated by Thwaites method and natural transition is predicted using Granville's correlation. If laminar separation occurs before transition, then the development of the laminar separation bubble is calculated using Horton's semiempirical technique. The development of the turbulent boundary layer and wake are calculated by the inverse formulation of Green's lag-entrainment method as outlined in the report by East et al.[6] Full details are given in the paper by Williams.[5]

Williams[7] has given a number of comparisons between his calculations and our experiments. Figure 11 shows how well his method can predict the pressure distributions even when there are large areas of separated flow on the upper surface. Figure 12 gives a more demanding comparison in which the measured and predicted transition points and separation points are plotted. The predicted transition often occurs through a short bubble rather than "naturally" as measured.

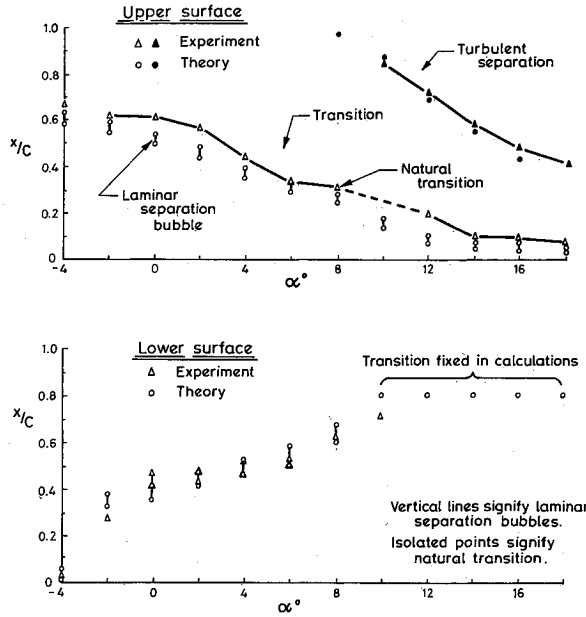

Fig. 12 Wörtmann FX63-137 transition and separation points, $Re_c = 0.7 \times 10^6$.

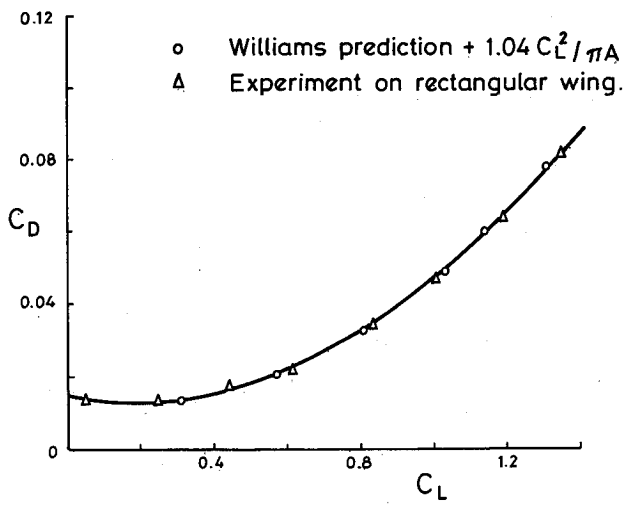

Fig. 13 Comparison between prediction and experiment, wing only $AR = 8.9$, FX63-137 section, and $Re_c = 0.7 \times 10^6$.

The measured transition positions are about 10%c ahead of the predicted values on the lower surface and about 10%c behind the predictions for the upper surface. However, the trends with incidence are forecast correctly and overall the predictions are reasonably good. The experimental measurements of transition position were made from surface oil-flow pictures. Titanium dioxide suspended in a mixture of linseed oil and paraffin was applied to the wing surfaces and the patterns photographed while the tunnel was running. Figure 13 compares the measured and predicted values of drag for the wing of the FX63-137 section with an aspect ratio of 8.9 at a Reynolds number of 7×10^5. The predicted values take the form drag as calculated by Williams and add the induced drag calculated by $C_{Di} = 1.04\ C_L^2/\pi A$. The prediction is in good agreement with the measured values. The greatest difference between the predicted and measured values of form drag (obtained from experiment by subtracting C_{Di}) is less than 0.002.

V. Conclusions

1) Of the airfoils tested, the FX63-137 and the Göttingen 797 achieved a high $C_{L\max}$ and good L/D ratios in the relevant Reynolds number range ($3 \times 10^5 < Re_c < 10^6$) for small RPV's.

2) Roughness strips degraded the performance of the three airfoils tested (NACA64_3-418, Gö797, and FX63-137), but the Wörtmann section was the least affected.

3) The computational fluid dynamics program developed by Williams is very useful. It can cope with the phenomena of laminar separation, transition, turbulent reattachment, and turbulent separation down to Reynolds numbers of 7×10^5.

4) Flight trials are very difficult in comparison with wind-tunnel tests. They demand extreme care and great perseverance. Nevertheless, the flight data are the final proof of the value of any modification. In our tests, the flight results confirmed the benefit of $C_{L\max}$ from changing the wing section. The drag measurements showed that excrescence and interference drag dominated the total drag figure and dwarfed the small benefits achieved by the wing alone.

Acknowledgments

Most of this research has been funded by the Ministry of Defence through the Royal Aerospace Establishment at Farnborough, whose help and advice is gratefully acknowledged. However, the views expressed are solely those of the authors.

References

[1]Render, P. M., "The Experimental and Theoretical Aerodynamics of Aerofoil Sections Suitable for Remotely Piloted Vehicles," Ph.D. Thesis, Cranfield, Inst. of Technology, England, 1984. See also: Render, P. M., Stollery, J. L., and Williams, B. R., "Aerofoils at Low Reynolds Numbers—Prediction and Experiments," *Numerical and Physical Aspects of Aerodynamic Flow—III,* edited by T. Cebeci, Springer-Verlag, New York, 1985, Chap. 8, pp. 155–167.

[2]Davidson, C. J., "The Experimental Investigation of the Effects of Roughness Upon Aerofoil Characteristics at Low Reynolds Numbers." M.Sc. Thesis, Cranfield Inst. of Technology, England, 1985.

[3]Trebble, W. J. G., "Low-Speed Wind-Tunnel Tests on a Full-Scale Unmanned Aircraft (X-RAE 1)," RAE TM Aero 2043, 1985.

[4]Schlichting, H., *Boundary-Layer Theory,* 6th Ed., McGraw-Hill, New York, 1968, Chap. 17, p. 512.

[5]Williams, B. R., "The Prediction of Separated Flow Using a Viscous-Inviscid Interaction Method," ICAS Paper 84-2.3.3, Sept. 1984; also Royal Aircraft Establishment TM Aero 2010, 1984.

[6]East, L. F., Smith, P. S., and Merryman, P. J., "Prediction of the Development of Separated Turbulent Boundary Layers by the Lag-Entrainment Method," Royal Aircraft Establishment TR 77045, 1977.

[7]Williams, B. R., "The Calculation of Flow About Aerofoils at Low Reynolds Number With Application to Remotely Piloted Vehicles," *Proceedings of the Conference on Aerodynamics at Low Reynolds Number* ($10^4 < Re < 10^6$), Vol. 3, Paper 29, Royal Aeronautical Society, London, 1986.